Structural and Electronic Properties of Amorphous and Polycrystalline In_2Se_3 Films

A. Chaiken,* K. Nauka, G.A. Gibson, Heon Lee,† and C.C. Yang

Hewlett-Packard

1501 Page Mill Rd.

Palo Alto, CA 94304

J. Wu, J.W. Ager, K.M. Yu, and W. Walukiewicz

Materials Sciences Division

Lawrence Berkeley National Laboratory

Berkeley, CA 94720

(Dated: March 19, 2003)

Abstract

Structural and electronic properties of amorphous and single-phase polycrystalline films of γ- and κ-In_2Se_3 have been measured. The stable γ phase nucleates homogeneously in the film bulk and has a high resistivity, while the metastable κ phase nucleates at the film surface and has a moderate resistivity. The microstructures of hot-deposited and post-annealed cold-deposited γ films are quite different but the electronic properties are similar. The increase in the resistivity of amorphous In_2Se_3 films upon annealing is interpreted in terms of the replacement of In-In bonds with In-Se bonds during crystallization. Great care must be taken in the preparation of In_2Se_3 films for electrical measurements as the presence of excess chalcogen or surface oxidation may greatly affect the film properties.

PACS numbers: 81.05.Hd, 68.55.Jk, 61.43.Dq, 64.70.Kb, 73.61.Jc

*Electronic address: chaiken@hpl.hp.com

†Now at Pohang University of Science and Technology, Pohang, Korea

I. INTRODUCTION

In_2Se_3 films have been studied as a precursor to $CuInSe_2$ for solar cells,[1] as an optical recording medium,[2] as a rotary polarizer for optoelectronics,[3] and, in Li-intercalated form, for battery applications.[4] The binary phase diagrams for III-VI compounds are complicated, and the unit cells of the III-VI crystal structures are large. This complexity originates from the many energetically similar ways that trivalent and divalent atoms can combine to satisfy their bonding requirements. In thin films a variety of different In-Se phases may be formed depending on the deposition method and parameters. For a given stoichiometry these phases differ primarily in the way that the cation vacancies are arranged.

In_2Se_3 crystallizes in the well-known layered (α-phase) or defect wurtzite (γ-phase) structures,[5] or a recently discovered anisotropic structure (κ-phase).[6] Ye *et al.* discovered large optical rotary power in what they term the vacancy ordered in screw form (VOSF) phase.[7] In layered compounds like α-In_2Se_3 or InSe, the cation vacancies form a plane, resulting in weak Se-Se bonding and anisotropic electronic properties.[8] In_2Se_3 and InSe are anisotropic hexagonal or rhombohedral semiconductors that tend to have a high resistivity.[9] In_4Se_3 on the other hand is a highly conducting smaller-bandgap orthorhombic semiconductor.[10] The higher conductivity of In_4Se_3 is attributed to the presence of In-In bonds, while in the other In-Se compounds indium bonds only to selenium.[11] The interpretation of electronic and optical data on polycrystalline thin films of the III-VI compounds is made more difficult by the frequent occurrence of more than one of these crystalline phases even in perfectly stoichiometric films.

Many different methods have been employed to prepare In_2Se_3 films, including coevaporation from elemental sources,[12] flash evaporation from the stoichiometric compound,[13] sputtering,[2] and even annealing of cold-deposited In/Se multilayers.[14–17] In this paper we describe structural, electronic, and optical characterization of In_2Se_3 films deposited by a number of methods and discuss how small quantities of impurity phases or slight surface oxidation can have a large impact on transport measurements. To the extent that they can be determined, the single-phase properties of unoxidized polycrystalline In_2Se_3 films are reported and compared to values in the literature.

II. EXPERIMENTAL METHODS

Indium-selenium films were deposited from the elemental constituents using either electron-beam sources or Knudsen cells in a chamber with a base pressure near 1x10^{-8} torr. $In_2Se_{3-x}Te_x$ ternaries were also studied. Zn, Si and Ge doping and Te alloying were accomplished using separate elemental sources. Substrate materials were either silicon or oxidized silicon, but the choice of substrates did not affect the films' composition or morphology. Deposition rates as measured by a quartz crystal were in the range of 0.1-1 nm/s and typical thickness was 400 nm. No dependence on deposition rate or thickness was noted. Substrates were optionally heated before, during or after deposition at temperatures up to 450 °C. The substrate temperature was monitored by a backside thermocouple in spring-loaded contact. Substrates that were not intentionally heated rose to a maximum of 60 °C during deposition; the resulting films are called "cold-deposited." For some samples, thin Al_2O_3 encapsulation layers were sputtered from an oxide target after indium selenide deposition. *Ex situ* post-annealing was performed in a tube furnace with a base pressure near 1x10^{-6} torr and plumbed with both 99.998%-pure Ar and an Ar-5%H_2 mixture.

Composition of the films was measured using energy-dispersive x-ray analysis (EDX) and Rutherford backscattering (RBS). Structural analysis was carried out using a four-circle x-ray diffractometer (XRD) and Cu Kα radiation. X-ray diffraction data are shown as semilog plots to emphasize the presence or absence of secondary phases. On selected samples transmission electron microscopy (TEM) was performed using standard techniques.[18] Cathodoluminescence measurements were performed in a Philips SEM using both photomultiplier and Ge detectors. Photoluminescence, photoreflectance and Raman spectroscopy were performed on some higher-quality films. The excitation energy for PL was 2.6 eV. Hall measurements were performed at room temperature using 4-lead and 6-lead geometries in a 1.2 T magnet. Metallic contacts for electrical measurements were made from sputtered Mo and were found to be linear for all but the most resistive films.

III. RESULTS

A. Composition and Crystal Structure

Polycrystalline indium-selenium films were produced using three distinct methods: coevaporation onto a heated substrate ("hot-deposited" films); coevaporation onto an unheated substrate followed by post-annealing ("cold-deposited" films); and deposition of an indium-selenium multilayer onto an unheated substrate, followed by post-annealing ("multilayer" films). The three types of depositions may be expected to favor different crystallization sequences and result in different microstructures and defects in the polycrystalline films. Post-annealing could be performed either in the deposition chamber ("in situ") or in the tube furnace ("ex situ"). When Ar-H_2 was used as the annealing gas, the two annealing methods produced identical results, as will be discussed further below. Finally, cold-deposited and multilayer films could be annealed either with or without the presence of an Al_2O_3 passivation layer. Below data for uncapped films are presented first.

Figure 1 shows conditions which produce the various phases of In_2Se_3, InSe and In for hot-deposited films. Phase purity was determined by x-ray diffraction. Holding the substrates at 125 °C to remove water vapor was not sufficient to induce crystallization, instead producing amorphous films. In general higher Se fluxes and higher substrate temperatures produced single-phase γ-In_2Se_3, although Se/In flux ratios over 2.0 and substrate temperatures under 300 °C resulted in incorporation of elemental Se into the films. Lower temperatures resulted in the formation of the recently discovered κ phase, which appears to be an analog of the α phase with reduced ordering.[6, 18, 19] The α phase was not observed in films deposited by any of the three methods.

The most surprising feature of Fig. 1 is that stoichiometric In_2Se_3 was reproducibly formed by growth under Se-deficient conditions. Annealing of cold-deposited uncapped films confirmed what was found in hot-deposited specimens, namely that large deviations from Se/In = 1.5 resulted in the presence of InSe or Se secondary phases, but small deviations could be corrected by annealing. Both EDX and RBS showed that In or Se excesses as large as a few percent could be removed by heat treatment either in vacuum or inert gas. Ternary films lost both excess Se and Te, with Te/Se ratios decreasing during annealing, consistent with previous reports.[20]

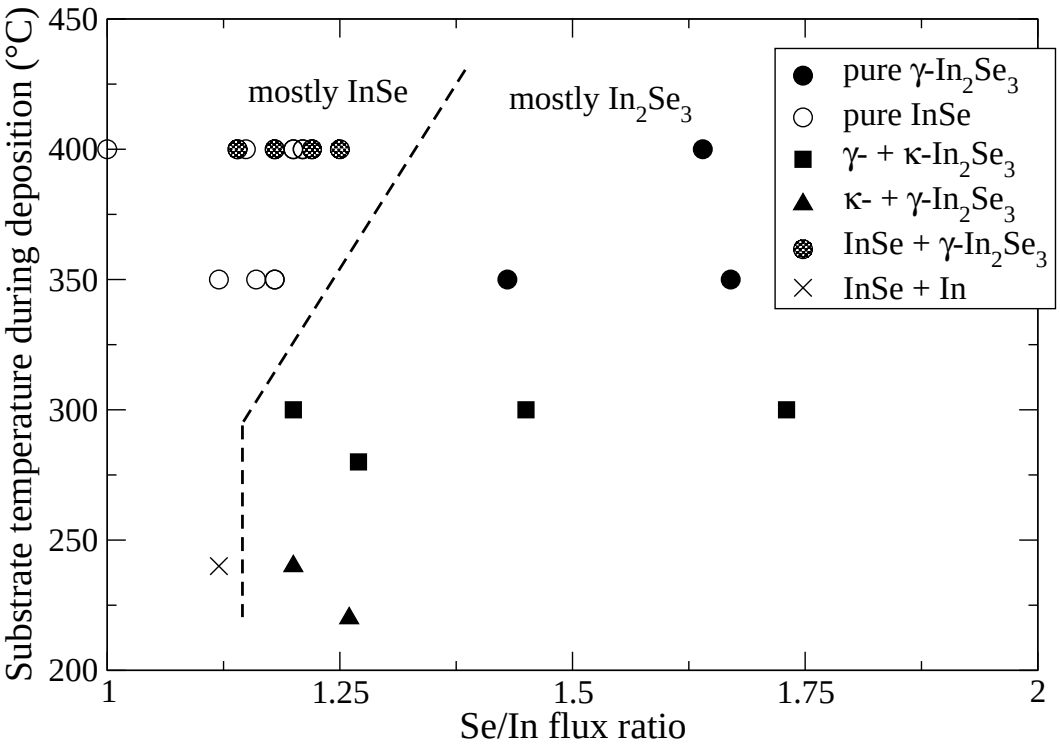

FIG. 1: Phase diagram of the Indium-Selenium system showing which compounds are produced as a function of substrate temperature and Se overpressure. "γ- + κ-In_2Se_3" means a film that is primarily γ-In_2Se_3 with κ as a minority phase. The dashed line is the separatrix between the fields where In_2Se_3 and InSe predominate.

Figure 2a shows a θ-2θ XRD spectrum for a typical hot-deposited pure γ-In_2Se_3 film that contains multiple crystallographic orientations. In contrast, Figure 2b shows the diffraction spectrum of an uncapped cold-deposited, co-evaporated *ex situ* annealed (350 °C, 30 minutes in vacuum) In_2Se_3 film. The single phase, complete (00ℓ) orientation and large grains are typical for cold-deposited, post-annealed films. X-ray diffraction on *in situ* post-annealed multilayer films (Figure 2c) indicates that they are fine-grained and contain some κ-In_2Se_3 crystallites, just like hot-deposited films. Figure 3 shows SEM images of the grains in hot- and cold-deposited co-evaporated films. Consistent with the x-ray diffraction results, the hot-deposited film consists of small grains of mixed orientation, while the post-annealed cold-deposited film is made up of large, flat $(00l)$-oriented platelets.

Quite different results have been found for cold-deposited capped films. RBS and EDX show that alumina (Al_2O_3) capping layers of 7 nm thickness suppress the evolution of volatile species, with the result that the composition of capped cold-deposited films did not change

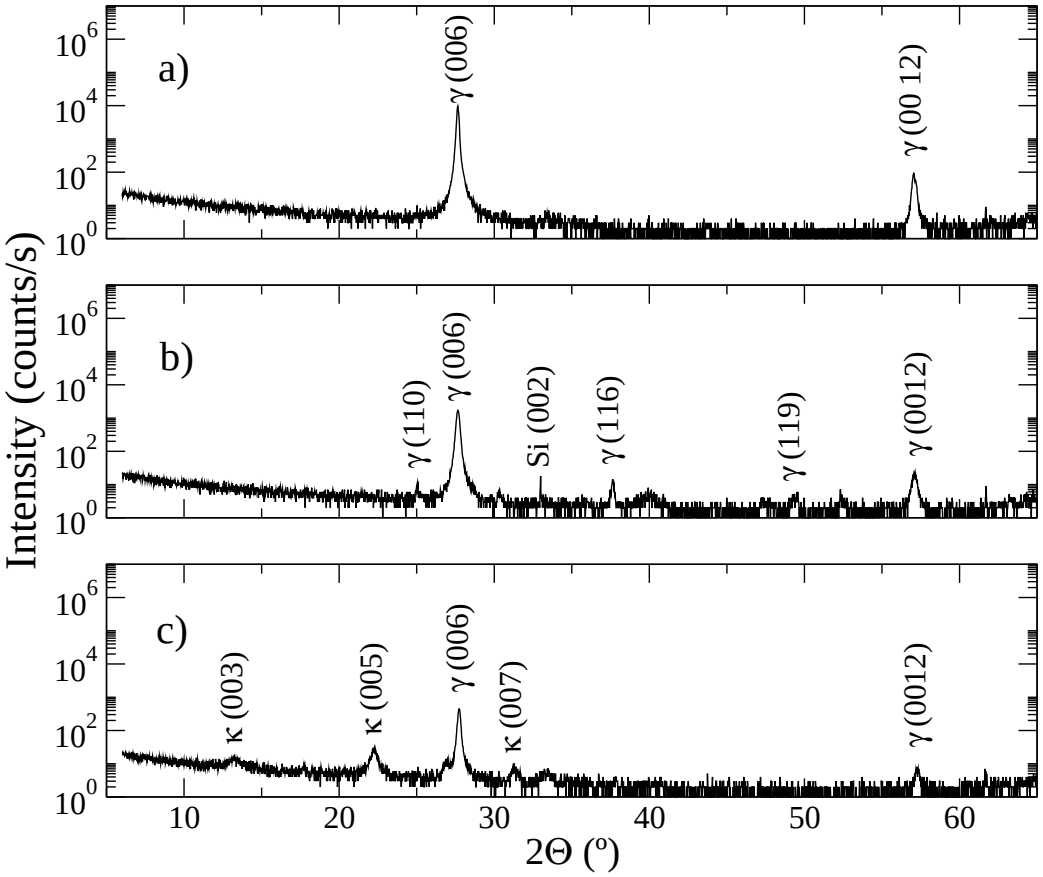

FIG. 2: X-ray diffraction spectra for typical In_2Se_3 films. a) A co-evaporated film deposited at 350 °C. b) A co-evaporated, cold-deposited film post-annealed at 350 °C for 30 minutes in vacuum. c) An In_2Se_3 film synthesized by annealing a cold-deposited (In 9.2 Å/Se 15.0 Å)x145 multilayer *in situ* at 400 °C for 30 minutes.

during annealing. Consequently while post-annealed uncapped films and *in situ* annealed films that are subsequently capped are often single-phase In_2Se_3, x-ray diffraction showed that post-annealed capped films typically contained small amounts of secondary phases, usually InSe or Se.

κ-In_2Se_3 occurred in films deposited at substrate temperatures in the 150 to 250 °C range, and in films that were deposited at lower temperatures and then annealed in the vacuum chamber. *Ex situ* annealed cold-deposited films may crystallize in the κ structure when annealed in an Ar-5%H_2 atmosphere, but never when annealed in Ar alone. These recent observations lend support to the idea[6] that surface oxidation and capping suppress formation of the κ phase. As shown in Fig. 4, further annealing of κ-phase films slowly

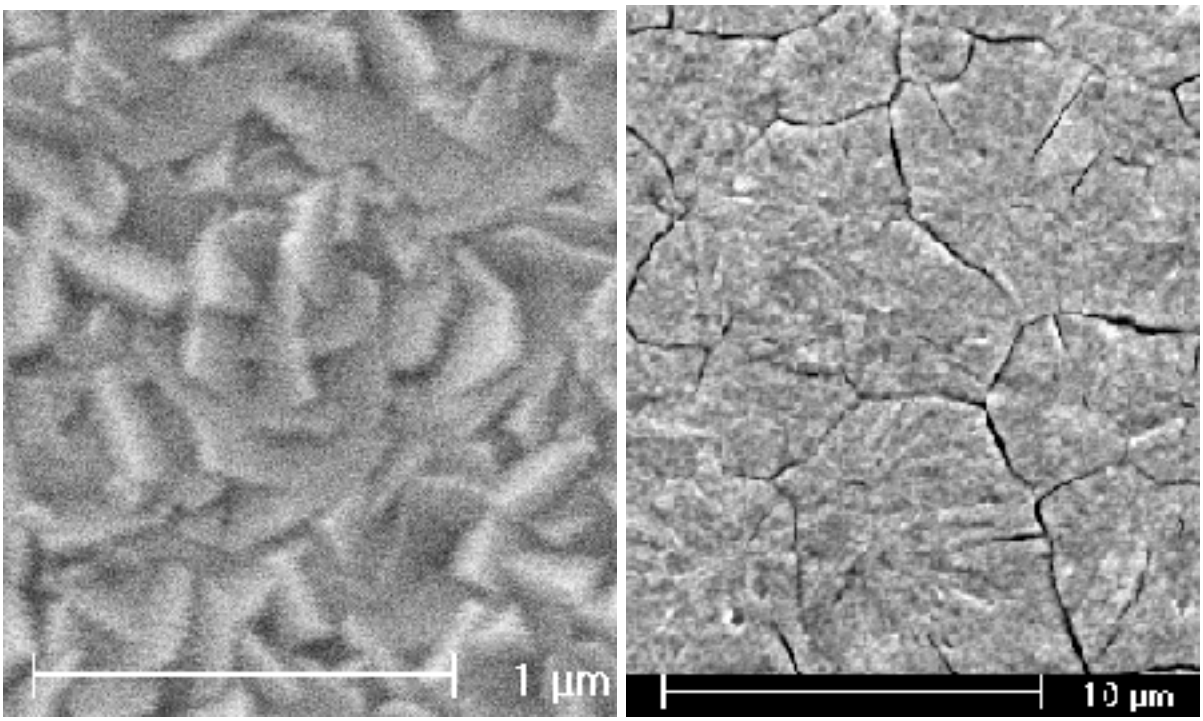

FIG. 3: SEM images of typical In_2Se_3 films. a) A co-evaporated film deposited at 350°C substrate temperature shows small tilted grains. b) A cold-deposited uncapped film *ex situ* annealed at 330 °C for 2 hours in Ar-H_2 shows large, plate-like grains.

transforms them into γ, suggesting that the κ phase is metastable. It's not clear if air exposure during acquisition of the first x-ray data shown in Fig. 4 played a role in the κ-γ transformation. Post-annealing has no effect on the microstructure of hot-deposited γ-phase films.

Zn doping in the range of 0.5-1% has permitted stabilization of a pure κ-In_2Se_3 film for the first time. Reference 6 reported that Ag doping stabilized the κ phase but with much broadened XRD peaks. Some peaks with similar d-spacings were reported for $In_2Zn_{0.4}Se_3$.[21] The XRD spectrum in Fig. 5 shows that all (00l) peaks appear, in contrast to the γ-In_2Se_3 spectrum, which typically shows only the (006) and (00 12) peaks. The κ spectrum has the unusual feature that odd-l (00l) peaks are more intense than even-l ones. Analysis of TEM diffraction patterns has yielded lattice constants $a = 8.09 \pm 0.10$ Å and $c = 19.85$ Å.[18] The latter value is in excellent agreement with the perpendicular d-spacing found by analysis of the XRD pattern.

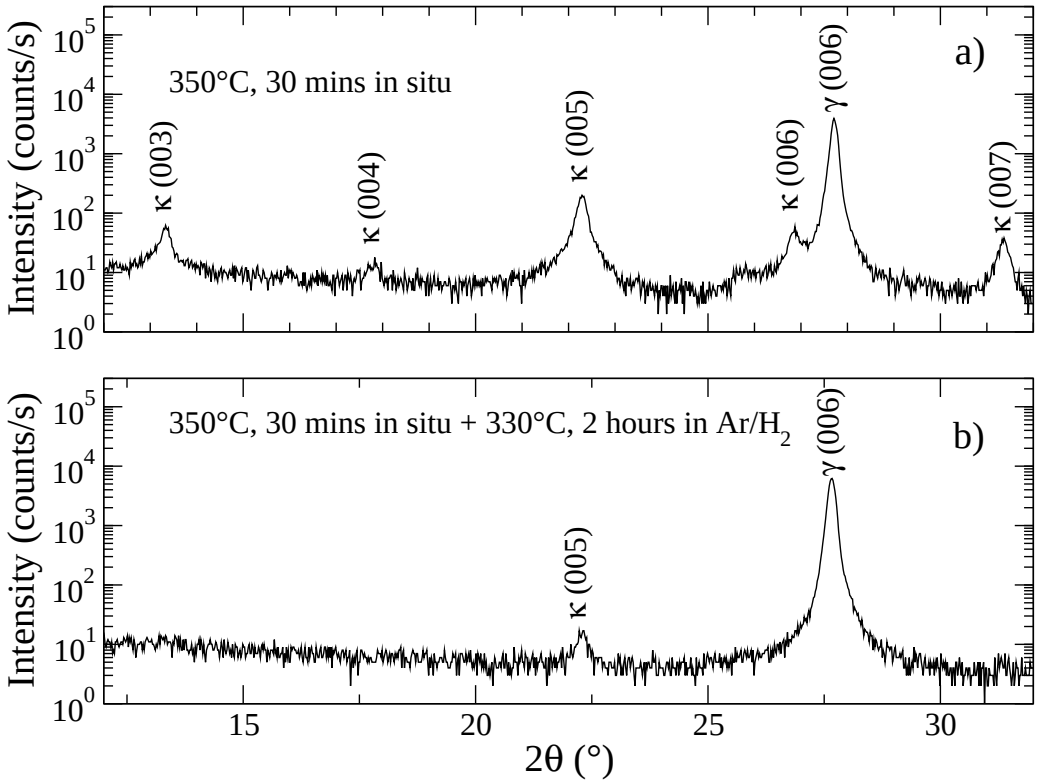

FIG. 4: X-ray diffraction spectra of a co-evaporated, cold-deposited In_2Se_3 film. a) After annealing at 350 °C for 30 minutes *in situ* after the deposition. Both γ and κ phases are present. b) After a further *ex situ* anneal of the same film in Ar/H_2 for 330 °C for 2 hours. The κ phase has been almost completely suppressed.

B. Resistivity and Hall Measurements

Figure 6 shows the results of transport measurements on a large number of In_2Se_3 films. Many other films were too resistive for successful Hall measurements. Except for the uncapped n-type films annealed in Ar and the capped p-type films, all the other data show that lower mobilities are correlated with higher carrier densities. X-ray diffraction and RBS show that all p-type films have excess Se or Te. Since polycrystaline Se is itself a relatively conducting p-type semiconductor,[22] it is likely that Se inclusions dominate the transport properties of these films. No p-type conduction was ever observed in uncapped films or in capped films that XRD, EDX and RBS showed to be stoichiometric. Similarly, the *in situ* annealed cold-deposited capped n-type films with high carrier density and low mobility were found by XRD to have inclusions of κ-In_2Se_3, as discussed further below. The presence of

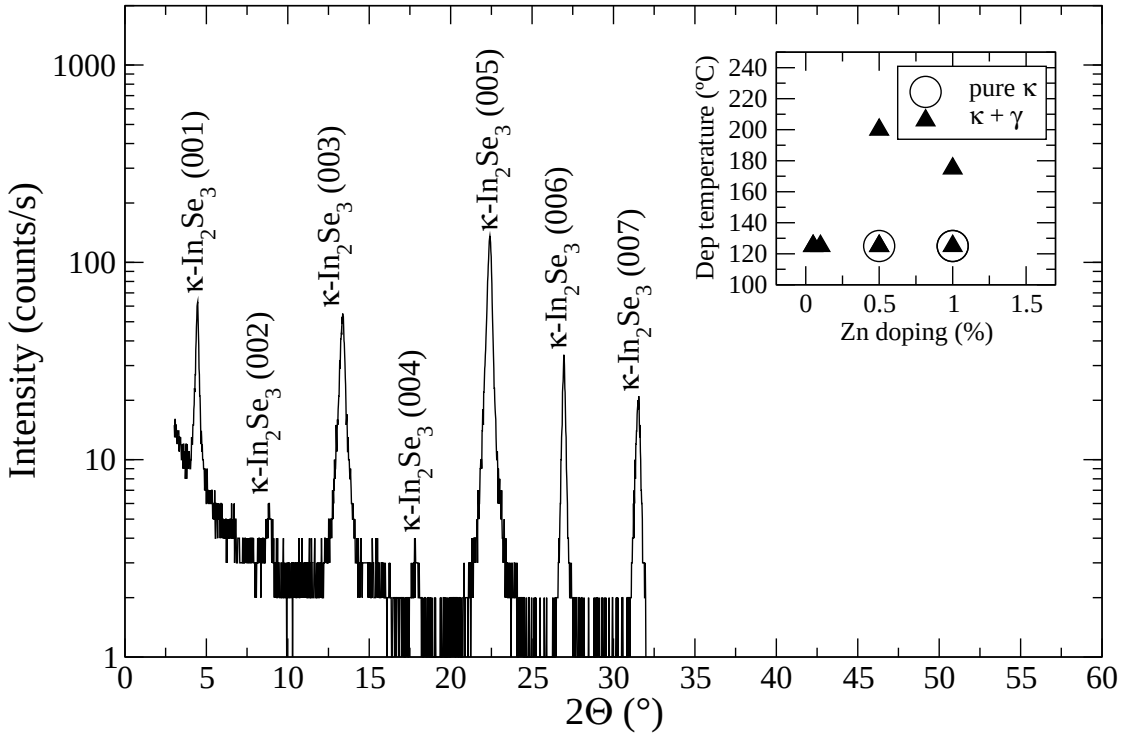

FIG. 5: X-ray diffraction spectrum of a film with nominal composition $In_2Zn_{0.01}Se_3$ deposited at 125 °C and then annealed *in situ* at 350 °C for 30 minutes. The presence of Zn allows formation of pure, well-ordered κ-phase. There were no peaks from the film above 32°. The inset shows the deposition temperature-Zn content conditions that yielded pure κ-phase films. All films were annealed to 350°C *in situ* after deposition.

InSe as a secondary phase did not affect the resistivity.

The high conductivity of the uncapped Ar-annealed films in Figure 6 appears to be explained by the presence of small amounts of In_2O_3, which is a degenerate n-type semiconductor.[23] On a few films very weak x-ray diffraction peaks matching the published d-spacings of In_2O_3 were observed. An experiment comparing top-contact and bottom-contact Hall measurements on a highly conducting uncapped film showed definitively that a surface layer was responsible for its low resistivity. The use of Ar:H_2 ambient rather than pure Ar prevented oxide formation. Unlike the slightly oxidized samples annealed in Ar, samples annealed in Ar:H_2 have characteristics similar to the uncapped, unannealed films and the *in situ* annealed capped films.

The remaining unexplained data points in Figure 6 are in the low carrier density, high mobility regime. Apparently these samples exhibit the intrinsic transport properties of γ-

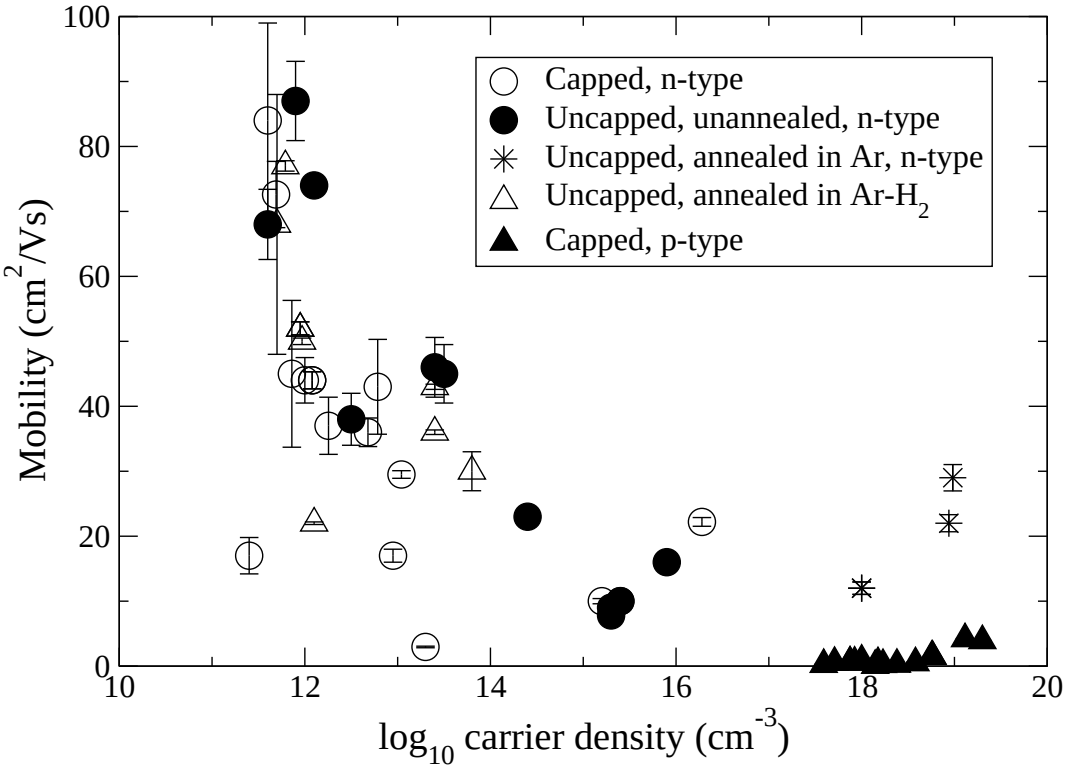

FIG. 6: A semilog plot of mobility versus carrier concentration for a number of In_2Se_3 films shows that higher carrier densities occur in films with lower mobilities. The errors originate from field-independent offsets in Hall measurements.

In_2Se_3 films, namely n-type carriers with density $< 10^{13}\text{cm}^{-3}$ and $20 \leq \mu \leq 60$ cm^2/Vs. No matter how films were deposited and no matter what their exact composition, texture or grain size, the transport properties of crystalline γ-phase films varied only slightly, as the data for capped γ-phase samples in Figure 7 illustrate.

Attempts at Si and Ge doping and annealing in a Se atmosphere did little to vary the carrier concentration as long as single-phase γ-In_2Se_3 was preserved. Tellurium alloying experiments followed the same trends, namely that capped films were p-type due to excessive chalcogen, while unoxidized uncapped films had a low carrier density and higher mobility. The dependence on Te content in n-type films with intrinsic behavior is quite weak, as illustrated by figure 8. Any variation in properties as a function of Te doping is smaller than the scatter in the properties of undoped films. Overall the properties of $In_2Se_{3-x}Te_x$ ternaries were minimally different from those of In_2Se_3 binaries with the same total chalcogen/In ratio.

Films containing κ-In_2Se_3 were significantly more conducting than those containing γ

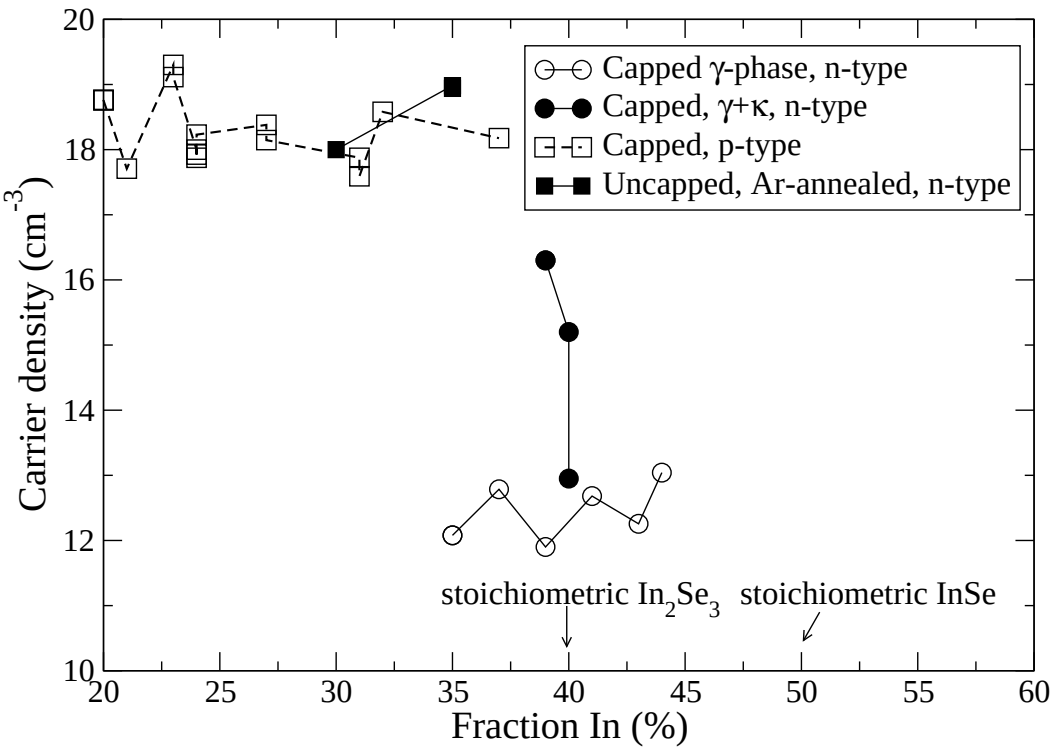

FIG. 7: The dependence of carrier type and density on composition illustrates the fact that only capped films with trapped excess chalcogens are p-type. Pure γ-phase films closer to stoichiometry are n-type with a lower carrier density, except for uncapped films which have a conducting oxide on the surface. Films with inclusions of κ-phase tend to have higher carrier densities. All compositions come from RBS or EDX measurements. The accuracy is estimated to be $\pm 1\%$.

phase only. Well-ordered single-phase κ films made with 0.5-1% Zn doping have a mobility $30 \leq \mu \leq 70$ cm^2/Vs and a carrier density of $5\text{x}10^{14} \leq \text{n} \leq 1\text{x}10^{16}$ cm^{-3}. Since Zn substituted on the In site should give p-type carriers, the Zn impurities are not acting as dopants, but may simply be serving to stabilize the more conducting κ phase. κ-containing films are not broken out in fig. 6, but are shown separately in figs. 7 and 9. Figure 9 demonstrates that conversion of κ-phase or amorphous material into γ as illustrated in fig. 4 can dramatically increase the resistivity. Prolonged annealing may also promote migration and clustering of defects. Surprisingly, annealing of well-crystallized nominally pure γ-phase uncapped films in an inert atmosphere invariably resulted in an increase in resistivity even though the x-ray diffraction spectra did not change.

Figure 10 shows the temperature-dependent conductivity of typical γ and κ films. There are two distinct temperature regimes. At temperatures above about 200 K, Arrhenius be-

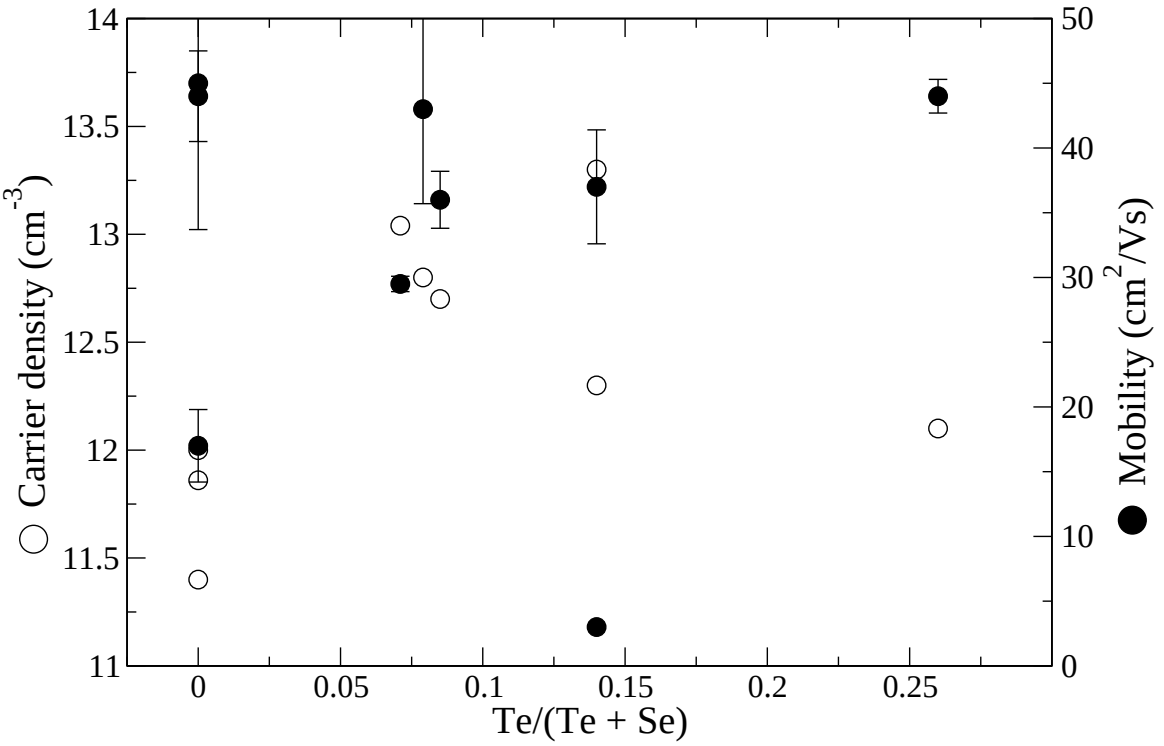

FIG. 8: Capped n-type $In_2Se_{3-x}Te_x$ film electrical properties do not show a trend with Te content. Zero-Te κ-phase films have been excluded.

havior is observed with an activation energy of 110 meV for γ and 70 meV for κ. These activation energies are much less than the reported bandgaps of 1.8-1.9 eV for the γ phase[6, 24] and 1.75 eV for κ,[6] implying that the carriers are derived from shallow defects. The conductivity saturates at lower temperatures where the carriers are frozen out. Yudasaka *et al.* reported activation energies between 130 and 780 meV depending on heat treatment of the γ-In_2Se_3 films.[9] Bernède et al. report activation energies between 0.20 and 0.75 eV depending on temperature of measurement and heat treatment of the film.[25]

C. Spectroscopic Measurements

Cathodoluminescence spectra for a well-ordered γ+κ-In_2Se_3 film are displayed in Figure 11. An additional broad, weak feature (not shown) is observed at about 1 eV. The peak at 1.915 eV corresponds to bandgap recombination for the γ phase and is in good agreement with previous studies of optical absorption on γ-phase films.[6, 24] The origin of the peak at 1.653 eV is unknown. The greater relative strength of the 1.653 eV peak at lower excitation

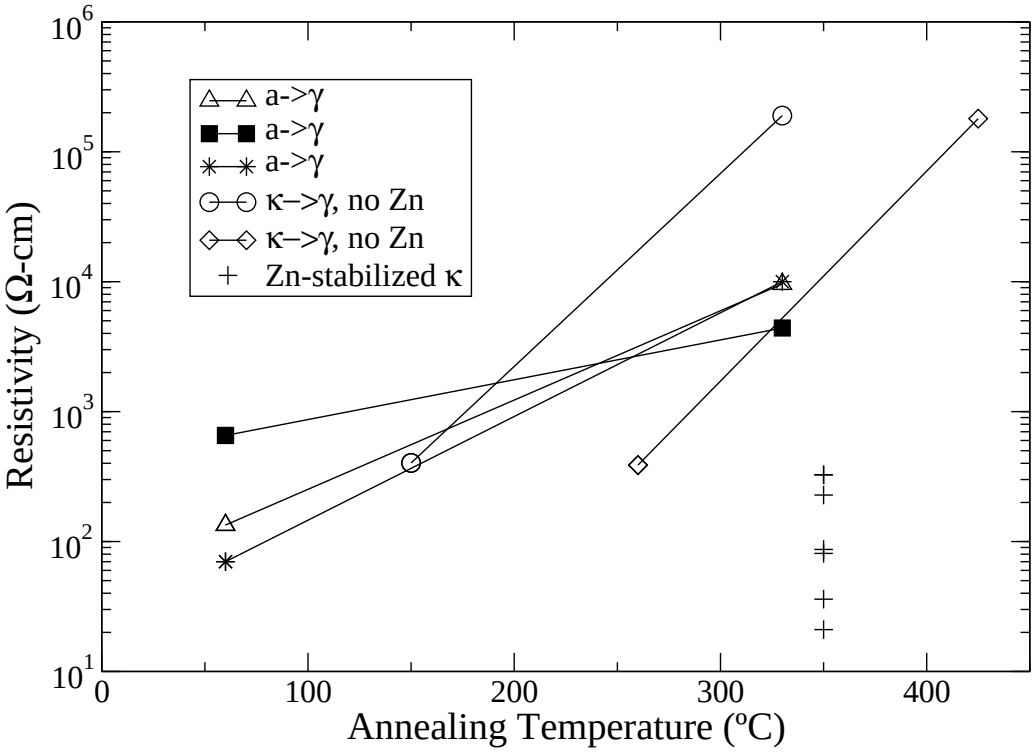

FIG. 9: Resistivity versus heat-treatment temperature for uncapped In_2Se_3 films. For pairs of point connected by a line, the left-hand point is as-deposited, and the right-hand point is for the same specimen after further *ex situ* annealing in Ar-H_2. The Zn-stabilized samples were deposited at 125 °C and annealed *in situ* to 350 °C. Films that x-ray diffraction showed to be amorphous (indicated as "a") actually had a lower resistivity than well-annealed γ-phase films irrespective of the grain size or texture of the polycrystalline material. Only κ-phase films retain a resistivity as low as the as-deposited state.

energy suggests that it derives from a defect with a higher concentration at the surface. The 1 eV peak presumably derives from a mid-gap defect band. Extensive study of the κ phase shows no CL signal.

Low-temperature photoluminescence spectra for two single-phase In_2Se_3 films are shown in Fig. 12. Both were doped with 1% Zn as determined by real-time flux measurements and confirmed by TEM/EDX. The κ film was deposited at 125 °C, while the γ was deposited at 175 °C under otherwise nominally identical conditions. Both were post-annealed to 350°C *in situ*. Each of the films shows what is likely band-edge PL near 2.11 eV, a larger value for γ than the CL measurement due to the lower measurement temperature of 11 K. The 2.11

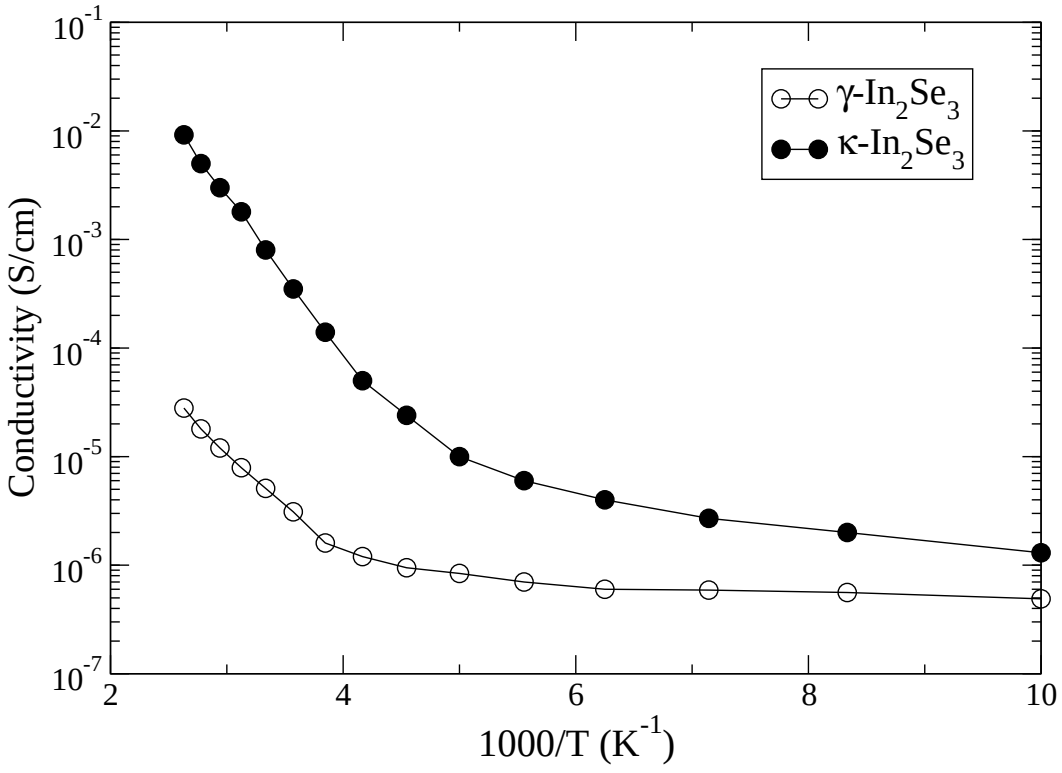

FIG. 10: The temperature dependence of the conductivity for typical γ- and κ-In_2Se_3 films shows two different regimes of behavior.

eV energy is consistent with the report by Ohtsuka *et al.* of CL peaks near 2.14 eV at 5 K in epitaxial In_2Se_3 films that likely are in the VOSF structure.[5]

The κ film has more mid-gap luminescence than the γ one. In addition the κ phase exhibits weaker peaks at 2.02 and 2.24 eV. Given the smaller reported bandgap of the κ phase[6] and its lack of room-temperature CL signal, it's possible that the feature at 2.12 eV in the κ spectrum is from a tiny amount of γ secondary phase that did not show up in the XRD spectrum of Fig. 5. In that case the κ-phase film shows no bandgap luminescence. The 2.02 and 2.24 eV PL peaks may both originate from defects.

IV. DISCUSSION

A. Phase Stability in In_2Se_3

Phase diagrams like Fig. 1 have appeared in several previous studies of the In-Se system. Brahim-Ohtsmane et al. found γ-In_2Se_3 in the 300-350°C temperature range and for 4 <=

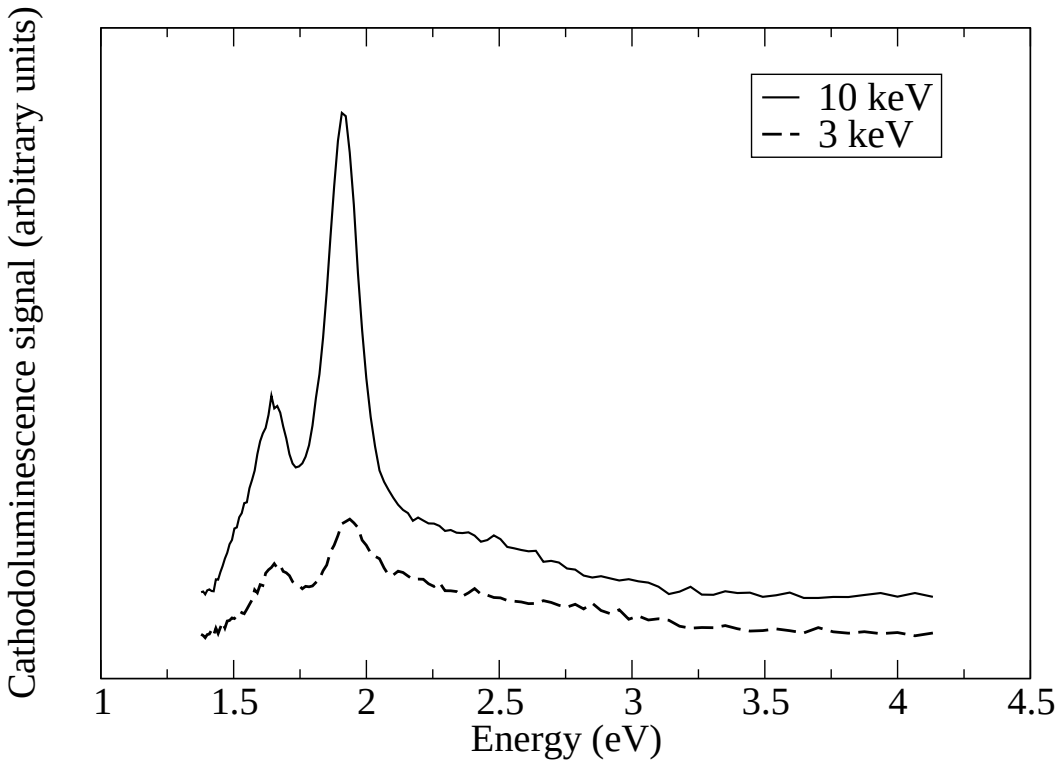

FIG. 11: Cathodoluminescence spectra at room temperature of a well-ordered γ-In_2Se_3 film taken at 10 keV and 3 keV electron-beam excitation energies. κ-In_2Se_3 exhibits no room-temperature cathodoluminescence.

Se/In <= 7.[12, 26] Yudasaka and coworkers observed the γ phase for 170° <= T_{sub} <= 300°C and 1.7 <= Se/In <= 9. Ohtsuka *et al.* produced single-phase γ-In_2Se_3 in the 300-550° temperature range and 5-15 Se/In flux range.[5] Ohtsuka *et al.* call their MBE films γ-In_2Se_3, but report seeing some of the extra (*hhl*) peaks[5] that Ye *et al.* have identified in single crystals as the VOSF phase.[7] Ye and coworkers say that the VOSF phase is stable at room temperature but is obtained from the high-temperature α phase only by long annealing times.[7] A long-period superlattice structure such as the VOSF is not likely observable in polycrystalline films. Various authors claim to see monoclinic In_6Se_7[9] or β- or δ-In_2Se_3, but single-phase films of these other structures are never obtained, making definite identification difficult.

None of the previous authors have reported formation of In_2Se_3 under Se-deficient conditions, although ZnSe films can be grown under both cation- and anion-rich fluxes.[27] Thermochemical calculations predict that the volatile species will be In_2Se on the In-rich

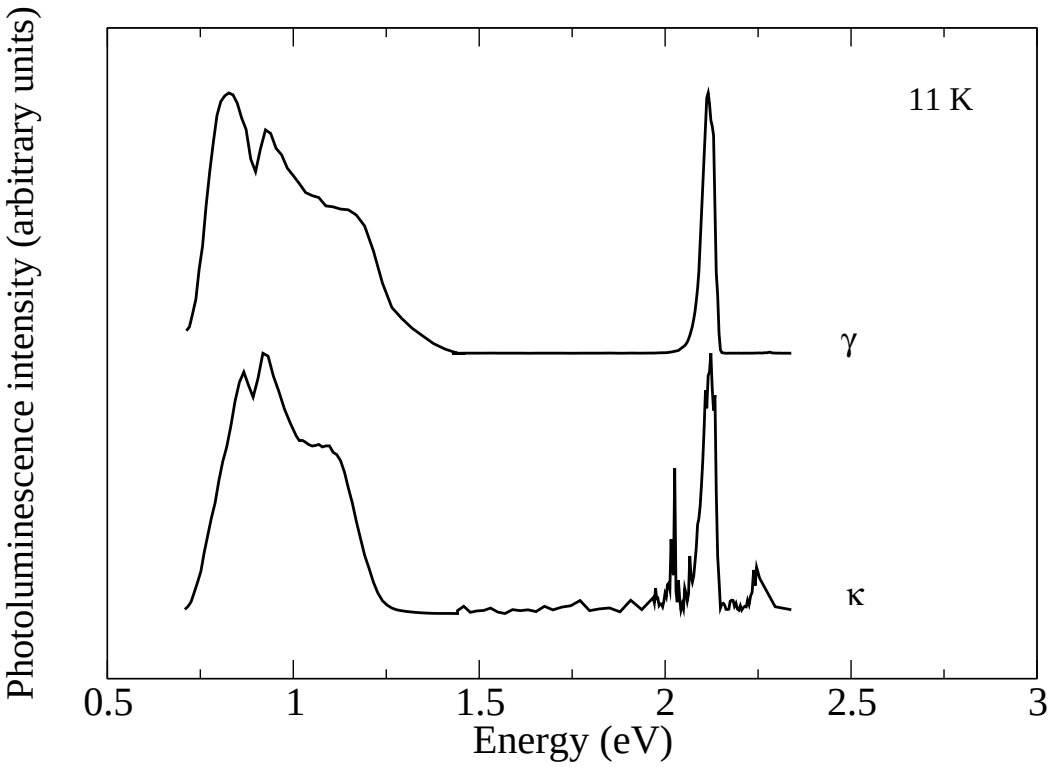

FIG. 12: Photoluminescence spectra of single-phase γ- and κ-In_2Se_3 at 11 K. The y-axes of the spectra have been normalized to the same scale for convenience. The data below and above 1.5 eV for each film were acquired separately and normalized. The dip near 0.9 eV is instrumental.

side of stoichiometry and Se polyatomic molecules on the Se-rich side of stoichiometry.[28] In_2Se evaporation has been invoked to explain In loss in sputtered $CuInSe_2$ films.[29] The fact that single-phase In_2Se_3 has been grown down to a Se/In ratio of 1.2 in the present study is consistent with the RBS and EDX findings that post-annealing of both Se-rich and In-rich films can drive them towards perfect stoichiometry.

One obvious question is, can we identify the κ phase with any of the previously identified In_2Se_3 structures, or is it truly novel? κ-In_2Se_3 has a bandgap and a $(00l)$ x-ray diffraction pattern similar to the VOSF phase, but its c-axis lattice constant is significantly larger. (See Table I.) The long-time annealing needed to produce the VOSF structure is opposite to the disappearance of the κ phase under similar conditions, as shown in Fig. 4. α-In_2Se_3 has a lamellar microstructure like κ and suggestively has half the a lattice constant, but once again the c lattice constant doesn't match. A careful comparison of the γ and κ structures shows clear differences.[18] The accumulated evidence of Table I therefore points to the conclusion

TABLE I: Properties of single-phase In_2Se_3 films and single crystals. NR = not reported. Lattice constants are from the International Center for Diffraction Data JCPDS files[30] unless otherwise noted. The in-plane lattice constant and PL measurements for κ were performed on a film with 1% Zn. Mid-gap PL and CL peaks are omitted. The 1.915 eV CL peak was measured at room temperature while the 2.14 eV CL peak and all the PL spectra were measured at low temperature.

Phase	a (Å)	c (Å)	Eg (eV)	CL Peak (eV)	PL Peak (eV)	ρ ($\Omega-$cm)	n (cm^{-3})	μ (cm^2/Vs)
γ	6.20	19.3	1.8[a]-2.0[b]	1.915, 1.65	2.11	10^4–10^6	10^{11}–10^{13}	20-60
α	4.025	19.235	1.36[c]	NR	1.523, 1.326[d]	10^3–10^5[e]	NR	NR
VOSF	7.1[f]	19.4[f]	1.70[f]	2.14[g]	NR	NR	NR	NR
κ	8.09[h]	19.8[i]	1.75[j]	none	2.13, 2.02, 2.45	10^2–10^3	10^{14}–10^{16}	40–50

[a]Ref. 24
[b]Ref. 9
[c]Ref. 31
[d]Ref. 32
[e]Ref. 33
[f]Ref. 7
[g]Ref. 5
[h]Ref. 18
[i]Ref. 6, 18
[j]Ref. 6

that the κ-In_2Se_3 is a newly identified phase, as previously claimed.[6]

If the κ structure is characteristic of an easily produced metastable phase, then why wasn't it observed in one of the many earlier studies on the In-Se system, beyond that of Haeuseler *et al.*[21] and deGroot and coworkers?[6] One reason is that κ forms only at low temperatures, as shown in Fig. 1, while MBE depositions are usually performed at higher temperatures. A second reason is the sensitivity of κ formation to the surface condition of the film. If κ nucleates at the surface of a growing film, then the small surface/volume ratio of single crystals may prevent the growth of measurable amounts of κ. Another possibility is that earlier investigators have thought that small amounts of κ-structure were In_6Se_7 since the two structures have several d-spacings in common. For example, the κ (200) and In_6Se_7 (111) both have d = 3.52Å. Yudasaka *et al.* report the formation of In_6Se_7 for substrate temperatures in the 100-300 °C range and 0.8 <= Se/In <= 1.4,[9] not that different from the formation range of κ-In_2Se_3 shown in Fig. 1.

B. Microstructure and crystallization

The features found in the x-ray diffraction spectra for uncapped In_2Se_3 depend almost entirely on thermal treatment and only weakly on the substrate, the Se/In flux for hot-deposited films or the Se/In starting composition for cold-deposited films. As Figs. 2 and 3 show, the crystallization of γ-In_2Se_3 is unusual in that post-annealing of cold-deposited films produces larger grains and a stronger $(00l)$ texture than hot depositions do even though the post-annealing temperature and hot-substrate temperature are both nominally 350 °C. During the annealing of amorphous films the nucleation of γ-phase must be slow and must be followed by rapid in-plane growth of grains. Analogous behavior is observed in In/a-Se multilayers, where films annealed at higher temperatures form smaller grains due to a exponential increase in the density of nuclei as a function of temperature.[17] In that case differential scanning calorimetry (DSC) and TEM studies show that nuclei of an orthorhombic phase form at Se/In interfaces during the cold deposition.[17] Lu and coworkers identify this orthorhombic phase as In_2Se,[17] but more recent work[10, 34] says that the orthorhombic structure is In_4Se_3. Lu *et al.* explain that the orthorhombic phase forms first since it has the highest effective heat of formation in the In-Se system. Subsequent anneals of the In/a-Se multilayers cause the In_4Se_3 nuclei to grow and to react with Se to form InSe and finally In_2Se_3.[17] While there are important differences in crystallization kinetics between the multilayer foils and the present co-evaporated films, it's quite likely that crystalline nuclei, possibly In_4Se_3, form during co-evaporation of In_2Se_3 onto cold substrates. In TEM studies Bernède *et al.* observed microcrystallites in cold-deposited co-evaporated In-Se films of various compositions, and found that the density of crystallites increased with increasing In content.[35] These microcrystallites were too small to generate any XRD features.[35] The nuclei must transform to In_2Se_3 and grow quite rapidly to impingement during the temperature-increase segment of an annealing process, preventing the nucleation of many smaller misoriented grains at higher temperatures. In hot MBE depositions, in contrast, many small In_2Se_3 grains must nucleate without the In_4Se_3 intermediate.

In the present work XRD results show that the grain size is not much affected by the choice of substrate or passivation layer, suggesting that nucleation of γ-In_2Se_3 occurs in the bulk of the film. Together with the observation that the presence of a cap layer prevents the formation of the κ phase, these results imply that capping suppresses the formation

of the κ structure rather than promoting the nucleation of the γ structure. The κ phase therefore likely nucleates at the surface of crystallizing films. Ohshima has previously shown that dielectric passivation layers can either enhance or suppress surface nucleation in post-annealed amorphous chalcogenide films.[36]

C. Transport Properties of Single-Phase γ-In_2Se_3 Films

The results of Figure 9 are initially surprising, as one would always expect amorphous films to have higher resistivity than polycrystalline ones. There are several processes going on during the annealing that help to explain the results. One is loss of excess In or Se, as observed by RBS and EDX and as predicted by thermochemical calculations of vapor pressures.[28] A second is the growth of crystalline nuclei present in the cold-deposited film and the transformation of other phases into In_2Se_3. The third is the formation of grain boundaries as growing grains impinge upon one another. The fourth is motion and possible clustering of point defects.

At this point a lack of direct experimental evidence precludes informed discussion about the role of impurities in limiting the conductivity of annealed films. The weak dependence of film resistivity on grain size and orientation in In_2Se_3 films appears to be opposite to the findings of Micocci *et al.*, who observed a strong dependence of transport properties on crystallite size that they attribute to scattering dominated by grain-boundaries.[37] In addition, Micocci and coauthors report that resistivity decreases with increasing annealing temperature, contrary to the data reported here. However, these authors observed bandgaps range from 1.4 to 1.65 eV,[37] smaller than the 1.9 eV consistently reported for the γ-phase[6, 24] and more consistent with α-In_2Se_3.[31] Given the weak relationship between film orientation, grain size and resistivity, it appears unlikely that grain boundaries dominate the resistivity of the polycrystalline films discussed here.

Reordering of bonds during annealing offer a more likely explanation for the trends of Figure 9. If the highly conducting In_4Se_3 phase does indeed form microcrystallites in a-In_2Se_3 films as suggested by the work of Lu[17] and Bernède[35], then a percolation network of such inclusions could greatly reduce film resistivity, as originally suggested by Marsillac and coworkers.[11] Even without the presence of In_4Se_3 nuclei, the amorphous film may have more In-In bonds than the polycrystalline one, especially if the film loses excess In during

the annealing. This explanation is consistent with the n-type behavior observed in almost all a-In_2Se_3 films. As Marsillac *et al.* point out, amorphous chalcogenide films are typically p-type due to the presence of a high density-of-states band of valence-alternating pairs.[11] They attribute the n-type behavior of amorphous indium selenides to the presence of an In percolation network. In the model where bond reordering during crystallization causes the resistivity increase, the relative independence of transport properties with respect to grain size is a natural result.

X-ray diffraction, SEM images, CL and PL measurements show that the γ-phase films in the present work are well-ordered and single-phase, comparable to those in the literature. The conclusion that single-phase γ-In_2Se_3 films are highly resistive appears to be in conflict with many previous reports of substantial conductivity. Similarly the new experiments have failed to produce p-type In_2Se_3 by Te doping. A careful re-examination of these reports of high conductivity shows that in many cases interpretation is made uncertain by surface oxidation, excessive chalcogens, the presence of secondary phases, or deposition on soda lime glass, which may act as a source of Na dopant. As mentioned above, oxidation leads to the formation of a thin conducting skin which can cause a false low resistivity reading. An excess of chalcogens can cause p-type conduction and very high carrier densities. Secondary phases like κ-In_2Se_3 have a much lower resistivity than γ. The role of Na in In_2Se_3 is only speculative, but Li doping is known to increase conductivity.[4] The one previous report of the resistivity of MBE-grown co-evaporated single-phase γ-In_2Se_3 polycrystalline films cites a value of 10^6 to 10^{10} Ω-cm.[9] The authors found that resistivity increased with annealing temperature,[9] in agreement with the present findings.

Unfortunately resistivity measurements on epitaxial γ-phase films have not yet been reported, although Ohtsuka *et al.* have observed $\rho \approx 10^4$-10^5 Ω-cm for epitaxial α-phase films.[33] This value is not that different from resistivities reported here on polycrystalline γ films. Further investigation is required in order to understand the fundamental mechanism of conduction in γ In_2Se_3. In particular the very low measured carrier densities currently lack a detailed explanation although point defects and compensation are likely involved.

V. SUMMARY

Elemental evaporation has been used to prepare single-phase films of In_2Se_3 in both the κ and γ phases. κ In_2Se_3 is a metastable phase that nucleates at the film surface, while γ is the stable phase that nucleates in the film bulk. κ In_2Se_3 is relatively conducting but has weak luminescence, while γ In_2Se_3 is highly resistive but shows strong CL and PL. The increase of γ film resistivity upon annealing can be explained in terms of the suppression of κ phase and reduction of the number of In-In bonds. Previous reports of high conductivity in γ In_2Se_3 films are interpreted in terms of excess chalcogen, surface oxidation or unintentional Na doping.

Acknowledgements We thank R.G. Walmsley, G.W. Burward-Hoy and H. Birecki of HP for design and construction of equipment and M.D. Flores of HP for help with film deposition. We thank J. Jasinski, W. Swider, J. Washburn and Z. Liliental-Weber of the National Center for Electron Microscopy at Lawrence Berkeley National Lab for the TEM work. We acknowledge useful discussions with R. Bicknell-Tassius, S. Naberhuis and T.E. Novet of HP, C.H. deGroot, now at University of Southampton, and P.E.A. Turchi of Lawrence Livermore National Lab. We thank Prof. J.C. Bernède for transmission of unpublished results.

[1] M. Contreras, A. Gabor, A. Tennant, S. Asher, and R. Noufi, Prog. Photovoltaics **2**, 287 (1994).

[2] T. Nishida, M. Terao, Y. Miyauchi, S. Horigome, T. Kaku, and N. Ohta, Appl. Phys. Lett. **50**, 667 (1987).

[3] J. Ye, T. Yoshida, Y. Nakamura, and O. Nittono, Appl. Phys. Lett. **67**, 3066 (1995).

[4] C. Julien, E. Hatzikraniotis, A. Chevy, and K. Kambas, Mater. Res. Bull. **20**, 287 (1985).

[5] T. Ohtsuka, K. Nakanishi, T. Okamoto, A. Yamada, M. Konagai, and U. Jahn, J. Appl. Phys. **40**, 509 (2001).

[6] C. deGroot and J. Moodera, J. Appl. Phys. **89**, 4336 (2001).

[7] J. Ye, S. Soeda, Y. Nakamura, and O. Nittono, Jpn. J. Appl. Phys. **37**, 4264 (1998).

[8] W. Jaegermann, A. Klein, and C. Pettenkofer, in *Electron Spectroscopies Applied to Low-Dimensional Materials*, edited by H. Hughes and H. Starnberg (Kluwer Academic Publishers, 2000).

[9] M. Yudasaka, T. Matsuoka, and K. Nakanishi, Thin Sol. Films **146**, 1987 (1987).

[10] C. Julien, A. Khelfa, N. Benramdane, and J. Guesdon, Mat. Sci. Eng. **B27**, 53 (1994).

[11] S. Marsillac, J. Bernède, and A. Conan, J. Mat. Sci. **31**, 581 (1996).

[12] J.-Y. Emery, L. Brahim-Otsmane, M. Jouanne, C. Julien, and M. Balkanski, Mat. Sci. Eng. **B3**, 13 (1989).

[13] J. Guesdon, B. Kobbi, C. Julien, and M. Balkanski, Phys. Stat. Sol. **102**, 327 (1987).

[14] S. Sahu, Thin Sol. Films **261**, 98 (1995).

[15] S. Marsillac, J. Bernède, R. L. Ny, and A. Conan, Vacuum **46**, 1315 (1995).

[16] O. Oyelaran, T. Novet, C. Johnson, and D. Johnson, J. Am. Chem. Soc. **118**, 2422 (1996).

[17] K. Lu, M. Sui, J. Perepezko, and B. Lanning, J. Mater. Res. **14**, 771 (1999).

[18] J. Jasinski, W. Swider, J. Washburn, Z. Liliental-Weber, K. Nauka, A. Chaiken, G. Gibson, and C. Yang, Appl. Phys. Lett. **81**, 4356 (2002).

[19] K. Nauka, A. Chaiken, G. Gibson, W. Walukiewicz, J. Ager, and K. Yu, in *International Conference on the Physics of Semiconductors* (2002).

[20] H. E. Maliki, S. Marsillac, J. Bernède, E. Faulques, and J. Wery, J. Phys. Cond. Matt. **13**, 1839 (2001).

[21] H. Haeuseler and M. Himmrich, Z. Anorg. allg. Chem. **535**, 13 (1986).

[22] S. Kasap, *The Handbook of Imaging Materials* (Marcel Dekker, 1998), chap. 9, 2nd ed.

[23] E. B. Ali, G. Sorensen, J. Ouerfelli, J. Bernède, and H. E. Maliki, Appl. Surf. Sci. **152**, 1 (1999).

[24] C. Julien, A. Chevy, and D. Siapkas, Phys. Stat. Sol. **118a**, 553 (1990).

[25] J. Bernède, S. Marsillac, and A. Conan, Mat. Chem. Phys. **48**, 5 (1997).

[26] L. Brahim-Otsmane, J.-Y. Emery, and M. Eddrief, Thin Sol. Films **237**, 291 (1994).

[27] D. Cammack, K. Shahzad, and T. Marshall, Appl. Phys. Lett. **56**, 845 (1990).

[28] C. Chatillon, J. Cryst. Growth **129**, 297 (1993).

[29] A. Rockett, T. Lommasson, P. Campos, L. Yang, and H. Talieh, Thin Sol. Films **171**, 109 (1989).

[30] Joint Committee on Powder Diffraction Standards, *PDF-2 Database*, International Center for Diffraction Data (2002).

[31] P. Becla, Z. Gumienny, J. Misiewicz, and J. Pawlikowksi, Optica Appl. **12**, 143 (1982).

[32] M. Balkanski, C. Julien, A. Chevy, and K. Kambas, Sol. State Comm. **59**, 423 (1986).

[33] T. Ohtsuka, T. Okamoto, A. Yamada, and M. Konagai, Jpn. J. Appl. Phys. **38**, 4131 (1999).

[34] T. Massalski, H. Okamoto, P. Subramanian, and L. Kacprzak, eds., *Binary Alloy Phase Diagrams* (ASM International, 1990).

[35] J. Bernède, S. Marsillac, A. Conan, and A. Godoy, J. Phys. Cond. Matt. **8**, 3439 (1996).

[36] N. Oshima, J. Appl. Phys. **79**, 8357 (1996).

[37] G. Micocci, A. Tepore, R. Rella, and P. Siciliano, Phys. Stat. Sol. **148a**, 431 (1995).